

# CFD Simulation of Enhancement Techniques in Flat Plate Solar Water Collectors

**Jafar Mehdi Hassan**

Mechanical Eng. Dep.  
University of Technology  
[Jafarmehdi1951@yahoo.com](mailto:Jafarmehdi1951@yahoo.com)

**Qussai J. Abdul-Ghafour**

Mechanical Eng. Dep.  
University of Technology  
[kaisyj@yahoo.com](mailto:kaisyj@yahoo.com)

**Mohammed F. Mohammed**

Mechanical Eng. Dep.  
University of Technology  
[mohammed2007msc@yahoo.com](mailto:mohammed2007msc@yahoo.com)

## Abstract

The present work is a numerical study of thermal performance of modified flat plate solar water collectors. Numerical simulations have been done by solving the governing equations (Continuity, Momentum and Energy) equations in the laminar regime, three dimensions by using the FLUENT software version (14.5). The effect of flow on temperature distribution of flat plate water collectors by inserting (twist strip with twist ratio (3), helical spring surrounding the solid shaft) inside riser pipes is numerically simulated and compared with solar collector without inserting device inside its riser pipes at flow rates of  $(100)\ell/h$ . The numerical simulation results show that the flat plate water, solar collectors with the inserted, twist strip and helical spring that's surround the solid shaft were higher enhancement of heat transfer than without inserted devices. The useful energy in case of twist strip is (10%) higher than the case of flat plate solar collector without enhancement device. Also, the case of helical spring is increased (6.8 %) than the twist strip, and (16.2%) than collector without enhancement device for the same mass flow rate.

**Keywords:** Flat plate, Enhancement Techniques

## 1. Introduction

A solar water collector is a special kind of heat exchanger that transfers solar radiant energy into heat. Flat plate solar collectors have been in common use for both domestic and industrial purposes. This may be due to a simple design and low cost. In industrial applications, a set of enhancement techniques is widely used to improve the performance of heat exchangers. Enhancement techniques can be classified into : additional devices which are incorporated into a smooth round tube (twisted tapes, helical spring, wire coil and wire mesh and artificial roughness such as surface modification of a smooth tube (corrugated and dimpled tubes) or manufacturing of special tube geometries (internally finned tubes) Herrero Marti'n [1] 2011. A large number of research investigations were undertaken both numerically and experimentally to enhance the thermal performance of flat plate solar collectors .

Chii-Dong and et.al, 2007 [2] used sheet-and-tube water heater in domestic water system. The collector efficiency of double-pass sheet-and-tube solar water heaters with attaching internal fins on tube wall and external recycle was investigated theoretically in this study. They found that with recycle operation and internal fins attached, the collector efficiency increases with increasing the recycle ratio  $R$ , number of fins attached  $N_f$ , inlet water temperature  $T_{fi}$  and mass flow rate and decreases with increasing number of pair ducts  $n$ . Jaisankar and et.al., 2009[3] investigated the heat transfer and friction factor characteristics of thermosyphon solar water heater with full length twist, twist fitted with rod and spacer at the trailing edge for lengths of (100, 200 and 300 mm). for twist ratio 3 and 5 has been studied. The experiment was carried out in outdoor condition facing south direction with a tilt angle of (18 degree) in India. They found that the maximum heat transfer and friction factor is obtained for minimum twist ratio (3). Also they found the heat enhancement in full length twisted tape is better than that the twist fitted with rod and spacer. Alireza Hobbi and Kamran Siddiqui in 2009 [4] Submit an experimental study to investigate the impact of heat enhancement devices on the thermal performance of single-tube flat-plate solar collector with a total area of  $(0.145\text{ m}^2)$ . Different passive heat enhancement devices that include twisted strip, coil-spring wire and conical ridges were studied. The flow rate of  $(0.132\text{ l/min})$  is close to the typical flow rates in either thermosyphon (natural). The results showed that the heat enhancement devices are ineffective in enhancing heat transfer rate in the studied range and geometry Nagarajan and et.al. in 2010 [5] Examined heat transfer and friction factor characteristics of solar parabolic trough collector fitted with full length twisted tapes inserts of twist ratios of (6, 8 and 10) have been presented. The transitional flow regime is selected for this study with the Reynolds number range from 1192 to 2534. The experimental data obtained were compared with those obtained from plain tube published data. The heat transfer coefficient enhancement for twisted inserts was higher than that for plain tube for a given Reynolds number. . Manjunath. M.S and et.al, 2011[6] Enhancement

of thermal performance using finned tubes in an economical unglazed solar flat plate collector using CFD simulation (Fluent 6.3.26). The flow domain consisted of an unglazed flat plate absorber plate with circular absorber tube connected below the absorber. The results showed that, use of serrated fins enhances the heat transfer from the absorber plate to the water in the absorber tube and improves the overall thermal performance of the collector. Use of optimal number of fins in the serrated fin configuration may further increase the heat transfer from the absorber plate to the water in the absorber tube due to increasing of surface area for convective heat transfer. Alberto García and et.al In 2013 [7] Investigated by designed to carry out simultaneously the characterization of two solar collectors, One of the solar collectors was modified inserting wire-coils within their risers, under the same operating (mass flow rate and inlet fluid temperature) and weather conditions. They found wire-coil inserts promoted an average increase in thermal efficiency from (14% to 31%) and an increase in the useful power collected with no additional pressure losses of up to ( 8-12%) for the values of mass flow rates investigated.

The objective of present study is using different enhancement device (twisted strip and helical spring surrounding the solid shaft full contact) inserted inside riser pipes of flat plate solar collector. Flow field in a flat plate solar collector with and without enhancement device under uniform heat flux has been analyzed. Also, study the effect of these inserted devices on improves the thermal performance. This technique has been tested theoretically by means of using Computational Fluid Dynamics (CFD) Fluent (14.5).

**2. Numerical Formulation**

**2.1 Problem statement and**

The system geometry of uniform header in the present work consists of eight riser pipes. These pipes are connected with two headers pipes, one in each end. The working fluid (water) flows through it with flow rates (100) ℓ/hr. (Basic geometry) as shown in fig. 1. Also the working fluid flows together with different types of enhancement device (twist strip and helical spring inside riser pipes). Absorbing plate was fabricated through the work of curve surrounds riser pipes to increase the surface area of contact between the plate and the riser pipes fig. 2. A twisted strip geometry is a metal strip of finite length twisted. The twist ratio is (the pitch is a distance required for the strip). A twisted strip geometry is rotate 180 deg.), as shown in fig. (3).

The twist ratio [8].

$$T_R = \frac{P}{W} \tag{1}$$

The twist strip is assumed in full contact with internal surface of the pipe, so that the width of the tape is taken the same as diameter of riser pipe, (w=10mm) and the tape length and thickness are (L= 1100 mm , t=0.7 mm). One of twisted ratio (TR=3) is used in present work. Another type of enhancement technique inserted helical spring (the pitch equal 10 mm ) and solid shaft (D=6 mm, L=1100 mm) at the center inside riser pipe) The helical spring surrounds the solid shaft full contact with internal surface of the pipe, the helical spring diameter (1mm) as shown in fig.(4). For all cases , the entire system geometry slope is (30 degree) . Numerical results obtained demonstrated that such a design would improve the heat transfer from the walls of riser pipes to the liquid and therefore would result in the hot water production capacity of the solar collector.

The following assumptions are made in the analysis:

- Steady state
- Incompressible flow
- Laminar flow
- Three dimensional.

Uniform heat flux.

**3. Numerical model**

In order to analyze flow field in flat plate solar collector with and without enhancement device (twist strip, helical spring surrounding the solid shaft) inside riser pipes of solar collector under heat flux, a solution of continuity, momentum as well as energy equation is required. The computational domain is meshed with control volumes built around each grid using GAMBIT (version 2.4.6), which is the preprocessor for FLUENT (version 14.5). Numerical simulation was carried out using steady state implicit pressure based solver which is an in-built in the commercially available software FLUENT (version 14.5) [9]. The governing partial differential equations, for mass momentum and energy equation are solved for the steady incompressible flow. The velocity-pressure coupling has been effected through SIMPLE algorithm (Semi Implicit Method For Pressure-Linked Equations) developed by Patankar S.V [10]. Second order upwind schemes were chosen for the solution schemes. Laminar flow condition was used. Three dimensional mesh generations is built as shown in fig.(5,6, and 7).

**3.1 Mean flow equations**

All the equations are presented in cartesian coordinate.

Continuity:

$$\nabla(\rho V) = 0 \tag{2}$$

Momentum equation

$$\frac{\partial}{\partial x_i}(\rho U_i U_j) = \frac{\partial \rho}{\partial x_i} + \frac{\partial}{\partial x_j} \left[ \mu \left( \frac{\partial U_i}{\partial x_j} + \frac{\partial U_j}{\partial x_i} \right) - \overline{\rho U_i U_j} \right] \quad (3)$$

Energy equation

$$\frac{\partial}{\partial x_j}(\rho U_j T) = \frac{\partial}{\partial x_j} \left[ \frac{\mu}{Pr} \frac{\partial T}{\partial x_j} - \overline{\rho U_j T} \right] \quad (4)$$

### 3.2 Boundary conditions and operating parameters

Inlet boundary condition is specified as velocity inlet condition (0.0221 m/s) depending on flow rate of the working fluid. The inlet temperature change with time, and that data fed from experimental. Outflow boundary condition is applied at the outlet. Wall boundary conditions are used to bound fluid and solid regions. In viscous flow models, at the wall, velocity components are set to zero in accordance with the no-slip and impermeability conditions that exist there. The interface between the water and the absorber tube is defined as wall with coupled condition to affect conjugate heat transfer from absorber tube to the water. A varying heat flux equivalent to the solar insolation is applied at the top surface of the absorber plate see table (2). The bottom and side surfaces of the absorber plate and the outer surface of the absorber tube are defined as wall with zero heat flux condition to affect insulated conditions. The material used for both absorber plate and the tube is copper. The input parameters used in the analysis are as shown in Table(1). The prediction of collector performance requires information on the solar energy absorbed by the collector absorber plate. The solar energy incident on a tilted surface can be found by [11] During the current study will be imposed the absorber energy from absorber plate a uniform heat flux. For the purpose of analysis of water solar collector, MATLAB computer program was used.

### 3.3 Calculation of Heat Flux

An estimated of absorbed solar radiation was developed to determine the performance of the solar collectors to develop best thermal energy conversion system, many important parameters and relations that are required in order to achieve the results of this study.

#### 3.3.1 Solar Radiation Calculations

This calculation involves the determination of the beam and diffuse radiation.

$$I_T = I_b + I_d \quad (5)$$

The component of beam radiation on a collector surface ( $I_b$ ) can be found for a certain incident angle by the following relation (ASHRAE 2005) [12].

$$I_b = I_{dn} * \cos\theta \quad (6)$$

$$I_{dn} = \left( \frac{A}{\exp\left(\frac{B}{\sin\alpha_s}\right)} \right) \quad (7)$$

Where:

$$\sin \alpha_s = \cos\phi * \cos\delta * \cos\omega + \sin\phi * \sin\delta \quad (8)$$

The value of (A) and (B) were calculated using the equations (9) and (10) [13].

$$A = 1158 * (1 + 0.066 * (\cos(Z))) \quad (9)$$

$$B = 0.175 * (1 - 0.2 * (\cos(Z1))) - 0.004 * (1 - (\cos(Z2))) \quad (10)$$

Where

$$Z = \left( 360 * \frac{n}{370} \right) \quad (11)$$

$$Z1 = 0.93 * n \quad (12)$$

$$Z2 = 1.86 * n \quad (13)$$

### 3.3.2 Diffuse Radiation Calculation

This component of solar radiation can be calculated as follows. [13]

For vertical or tilt surface:

$$I_{ds} = Y.C.I_{dn} \quad (14)$$

Where:

Y: the ratio of sky diffuses radiation on vertical surface to that on horizontal surface.

C: dimensionless value represent to the average ratio of diffuse to normal beam radiation.

$$Y = 0.55 + 0.437 * \cos\theta + 0.313 * \cos\theta^2 \quad (15)$$

$$C = 0.0965 * (1 - 0.42 * \cos(z)) - (0.0075 * (1 - \cos(1.95 * n))) \quad (16)$$

Ground reflected radiation can be found form expression below: [14]

$$I_{dg} = 0.5 * r_g * I_{dn} * (C + \sin(\alpha_s)) * (1 - \cos(\beta)) \quad (17)$$

Where:

$r_g$ : the ground reflectivity = 0.4 [14]

$$I_d = I_{dg} + I_{ds} \quad (18)$$

### 3.3.3 Radiation Transmission Thorough Glazing Cover (Absorbed radiation)

The prediction of collector performance requires information on the solar energy absorbed (S) by the collector absorber plate. The solar energy incident on a tilted surface can be found by [11]

$$S = (I_b * R_b * \tau\alpha_b) + I_d * \tau\alpha_d * \frac{1 + \cos(\beta)}{2} + r_g * \tau\alpha_g * \frac{1 - \cos(\beta)}{2} \quad (19)$$

Where  $(\tau\alpha_b), (\tau\alpha_d), (\tau\alpha_g)$  are the transmittance-absorptance product for beam, diffuse and ground-reflected radiation components. The transmission, reflection, and absorption of solar radiation by the various parts

of a solar collector are important in determining collector performance. The transmittance, reflectance, and absorptance are functions of the incident solar radiation ( $IT$ ), glass thickness ( $L$ ), refractive index of glass cover ( $n$ ), extinction coefficient of the material ( $KL$ ), and number of glass cover ( $N_g$ ). When a beam of radiation strikes the surface of a transparent plate at angle,  $\theta_1$  called the radiation incidence angle. Part of the incidence radiation is transmitted through the glass cover and the remainder is refracted to angle  $\theta_2$ , which called the radiation refraction angle. Angles  $\theta_1$  and  $\theta_2$  are not equal when the density of the plane is different from that of the medium through which the radiation travels. The two angles are related by [11].

$$\frac{n_2}{n_1} = \frac{\sin\theta_1}{\sin\theta_2} \tag{20}$$

Where  $n_1$  and  $n_2$  are the refraction indices. A typical value of the refraction index is (1.526) for glass as used in this present work. Expressions for perpendicular ( $r_{1b}$ ) and parallel ( $r_{2b}$ ) components of radiation for smooth surfaces were derived by Fresnel law, [11] as follows:

$$r_{1b} = \frac{\sin(\theta_2 - \theta_1)^2}{\sin(\theta_2 + \theta_1)^2} \tag{21}$$

$$r_{2b} = \frac{\tan(\theta_2 - \theta_1)^2}{\tan(\theta_2 + \theta_1)^2} \tag{22}$$

Where

$$\theta_1 = \theta$$

$$\theta_2 = \sin^{-1}\left(\frac{\sin\theta_1}{N}\right) \tag{23}$$

Where

$N_g$ : Number of glass cover, in present work

$N_g = 1$  Similarly, the transmittance can be calculated from the above two components as follows [13]:

$$\tau_{nb} = 0.5 * \left( \left( \frac{1-r_{2b}}{1+r_{2b}} \right) + \left( \frac{1-r_{1b}}{1+r_{1b}} \right) \right) \tag{24}$$

The transmittance,  $\tau_{ba}$ , (subscript  $a$  indicates that only absorption losses are considered), can be calculated as [11]

$$\tau_{ba} = \exp\left(\frac{-k_1}{\cos\theta_2}\right) \tag{25}$$

Where  $K_1$  is the extinction coefficient (which can vary from 4 m<sup>-1</sup> for low quality glass, to 32m<sup>-1</sup> for high quality glass), and  $L$  is the thickness of the glass cover. ( $k_1=0.037$ ) [11] Then, the total transmittance for a beam radiation component becomes:

$$\tau_b = \tau_{ba} * \tau_{nb} \tag{26}$$

The proper transmittance ratio  $\alpha/\alpha_n$  can then be obtained from the following equation depending on the angle of incident of beam radiation component ( $\theta_i$ ) can be obtained from [13]. As follows:

$$\alpha = \alpha_n * ((1 - (1.5879 * 10^{-3} * \theta) + (2.7314 * 10^{-4} * \theta^2) - (2.3026 * 10^{-5} * \theta^3) + (9.0244 * 10^{-7} * \theta^4) - (1.8000 * 10^{-8} * \theta^5) + (1.7734 * 10^{-10} * \theta^6) - (6.9937 * 10^{-13} * \theta^7)) \tag{27}$$

$$\tau_{ab} = 1.01 * \tau_b * \alpha \tag{28}$$

For a given collector tilt angle, the following empirical relations can be used to find the effective angle of incidence of diffuse ( $\theta_d$ ) and ground-reflectance ( $\theta_g$ ) radiation can be estimated as follows [ 11]:

$$\theta_g = 90.0 - (0.5788 * \beta) + (0.002693 * \beta^2) \tag{29}$$

$$\theta_d = 59.7 - (0.1388 * \beta) + (0.001497 * \beta^2) \tag{30}$$

$$\alpha_g = \alpha_n * ((1 - (1.5879 * 10^{-3} * \theta_g) + (2.7314 * 10^{-4} * \theta_g^2) - (2.3026 * 10^{-5} * \theta_g^3) + (9.0244 * 10^{-7} * \theta_g^4) - (1.8000 * 10^{-8} * \theta_g^5) + (1.7734 * 10^{-10} * \theta_g^6) - (6.9937 * 10^{-13} * \theta_g^7)) \tag{31}$$

$$\alpha_d = \alpha_n * ((1 - (1.5879 * 10^{-3} * \theta_d) + (2.7314 * 10^{-4} * \theta_d^2) - (2.3026 * 10^{-5} * \theta_d^3) + (9.0244 * 10^{-7} * \theta_d^4) - (1.8000 * 10^{-8} * \theta_d^5) + (1.7734 * 10^{-10} * \theta_d^6) - (6.9937 * 10^{-13} * \theta_d^7)) \tag{32}$$

Where ( $\theta_g$ ) and ( $\theta_d$ ) are the effective incidence angle in (degrees) for diffuse radiation and ground reflectance components respectively. ( $\alpha_n$ ) is the absorptance at normal incidence angle, which can be found from the properties of the absorber cover. In this work this value is equal (0.9) for three radiation components as mentioned in literature. Now, the total transmittance-absorptance product for diffuse and ground reflectance radiation components can be estimated in same manner that estimated for beam radiation component, after using  $\theta_g$ , and  $\theta_d$  as the new incident angles for diffuse and ground reflectance components from Eq. (20) to (28). Subsequently, Eq. (28) can be used to find  $\tau_{ad}$  and  $\tau_{ag}$ . Finally, each value of transmittance absorptance product for three incident radiation components are substituting in eq. (19) to find the net absorbed radiation on collector surface see fig(19). For surfaces located at the northern hemisphere as mentioned at this paper, the collector must be sloped towards the equator (zero azimuth angles). Then the beam radiation tilt factor  $R_b$  was calculated as follows [11].

$$R_b = \frac{\cos\theta}{\cos\theta_z} \tag{33}$$

$$\cos\theta_z = \cos\phi * \cos\delta * \cos\omega + \sin\phi * \sin\delta \tag{34}$$

$w$  is the solar hour angle (degree), which can be estimated from the following equation such that [11]:

$$\omega = 15 * (AST - 12.00) \tag{35}$$

Where AST is the apparent solar time, which means the sun position before, after, and at local solar noon (when the sun at meridian of the observer). So the hour angle has a negative value before local solar noon, positive value after local. Solar noon and zero at local solar time (when AST = 12: 00 noon).

## 4. Result and Discussion

### 4.1 Velocity contour

Fig. (8) shows the secondary flow (swirl flow) create along the path of the riser pipe. That's leads two longitudinal vortices are generated around the twist strip. Also, inserting twist strip inside riser pipes decreases the hydraulic diameter and increases the fluid flow along the path of riser pipe. The maximum velocity gradient occurs near the wall in case of inserting helical spring surrounding solid shaft, because of the location of solid shaft at the center of the pipe force the fluid to move around it as shown in Fig. (9). The velocity magnitude near the pipe wall due to inserted helical spring surrounding solid shaft is increased by (64%) than riser pipes without inserting devices and (52%) than riser's pipes with inserted twisted strips That's due to the hydraulic diameter in this case is less than twist strip that's leads to increase the fluid flow from the reign bounded between solid shaft and inner tube wall. Also, the helical spring create swirling flows along the path of riser pipe that modify the near wall velocity profile due to the various vortices distributions in the vortex core as shown in Fig's (10),(11) and (12).

### 4.2 Temperature contour

Fig's (13),(14) and (15) show the temperature distribution of absorber plate of flat plate solar collectors with and without inserted enhancement device. In general, the temperature distributions of the absorber plate increase gradually to the direction of flow inside riser pipe. The absorber plate temperature of the flat plate water solar collector without inserting enhancement device is higher than the others. Because of inserted enhancement device inside riser pipes leads to increase the heat transmitted from the absorber plate to the fluid that leads finally to reduce the absorber plate temperature. In fig's (16) to (18) shows the water temperature distribution inside risers pipes for the mass flow rate of order (100) l/hr. for three different sections at (Z=10 cm, Z=50cm and Z=90cm) for with and without inserting enhancement device to show the temperature distribution of water inside riser

pipes at these sections . In general the water temperature was increases in the direction of flow inside riser pipes. The results show that the water temperature in case of inserted helical spring is higher than the others for the same mass flow rates. Also, in case of inserted twist strips inside riser pipes show the water temperature is higher than in case of risers without inserting device for the same mass flow rates. That's due to the enhancement devices leads to increase the velocity near the wall pipe due to swirl generation effects and finally increase the heat transfer coefficient inside riser pipes.

### 4.3 Useful energy

Fig (20) shows the useful energy of flat plate solar water collectors with and without enhancement device inside riser pipes for the same mass flow rate. It is clear that, the useful energy in case of inserted helical spring surrounding solid shaft inside riser pipe is higher than the others. Also, the useful energy in case of twist strip is (10%) higher than the case of flat plate solar collector without enhancement device. Also, the case of helical spring is increased (6.8%) than the twist strip, and (16.2%) than collector without enhancement device .The numerical results as compared with experimental results [15] with error not exceeds (16%)

## 5. Conclusion

- The numerical simulation of flat plate water solar collectors with inserted twist strip and helical spring surrounding the solid shaft give higher enhancement of heat transfer than without inserted device inside riser pipes due to increased velocity distribution near the wall.
- The velocity distribution in case of inserted helical spring surrounding the solid shaft is more uniform than other .
- The insert of helical spring surrounding the solid shaft inside riser pipes gave higher enhancement of heat transfer than the others for the same mass flow rate.

## 6. Nomenclature

Symbol	Title
I	Hourly solar radiation (J)
$I_b$	Beam hourly solar radiation (J)
$I_d$	Direct hourly solar radiation (J)
$I_T$	Total Hourly solar radiation (J)
$N_g$	Number of glass cover
n	Number of days in the year
P	Pitch (mm)
$Q_U$	Useful energy (watt)
rg	the ground reflectivity
$T_R$	Twist ratio

w	Strip width (mm)
Y	The ratios of sky diffuse radiation on vertical surface of that on horizontal surface
$\tau\alpha$	Effective transmittance-absorptance
$\phi$	Latitude angle (degree)
$\delta$	Declination angle (degree)
$\gamma$	Surface azimuth angle (degree)
$\beta$	Surface tilt angle (degree)
$\omega$	Hour angle (degree)
$\theta$	Incidence angle (degree)
$\theta_z$	Reflected angle (degree)
$\theta_g$	Effective angle of ground reflectance
$\theta_d$	Effective angle of incidence of diffuse
$\theta_z$	Zenith angle (degree)
$\alpha$	Solar absorptance
$\alpha_s$	Solar altitude angle (degree)
$\gamma_s$	Solar azimuth angle (degree)
$\tau\alpha_b$	Transmittance-absorptance for beam radiation
$\tau\alpha_d$	Transmittance-absorptance for diffuse radiation
$\tau\alpha_g$	Transmittance-absorptance for ground radiation

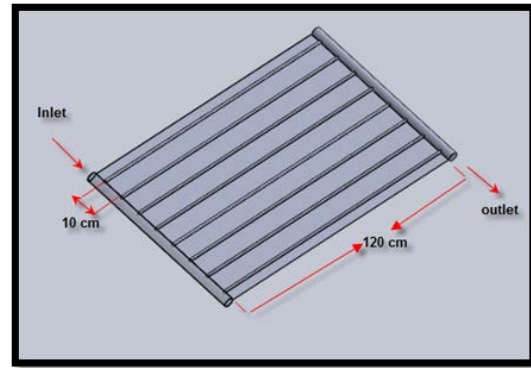
Table (1): input parameter for simulation

Parameter	Value
Density (Copper)	8978 kg/m <sup>3</sup>
Specific Heat (Copper)	381 J/kg-K
Thermal Conductivity (Copper)	386 W/m-K
Density (Water)	998.2 kg/m <sup>3</sup>
Viscosity (Water)	0.001003 kg/(m.s)
Specific Heat (Water)	4182 J/kg-K
Thermal Conductivity (Water)	0.6 W/m-K

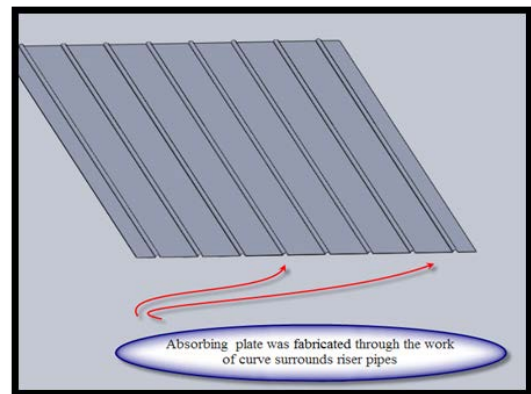
Source: Manjunath et al. (2011) [6]

Table (2): Variation of heat flux with time of day

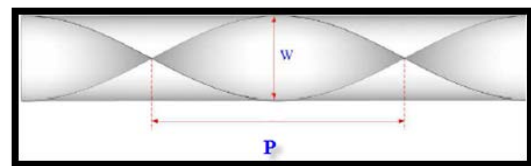
No.	Time	Heat flux W/m <sup>2</sup>
1.	8.00am	283.4391
2.	9.00am	491.3378
3.	10.00am	654.3232
4.	11.00am	759.56
5.	12.00 noon	796.6242
6.	1.00 pm	759.56
7.	2.00pm	654.3232
8.	3.00pm	491.3378
9.	4.00pm	283.4391
10.	5.00pm	89.618



Figure(1): Basic geometry Z-Configuration



Figure(2): Absorbing plate geometry



Figure(3): Typical twisted tape geometry

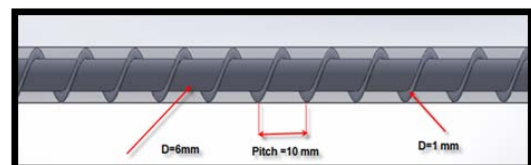
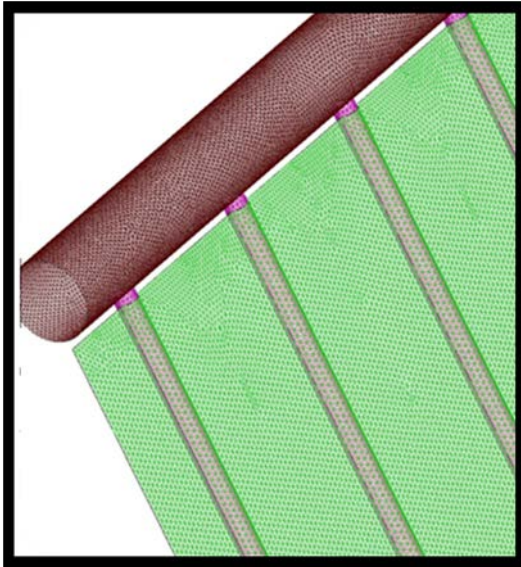
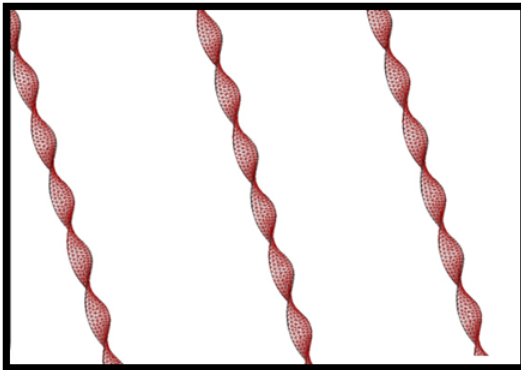


Figure (4): Helical spring surrounding solid shaft geometry inside riser pipe



**Figure (5):** Volume mesh for uniform headers flat plate solar collectors.



**Figure (6):** Volume mesh of twist strip geometry

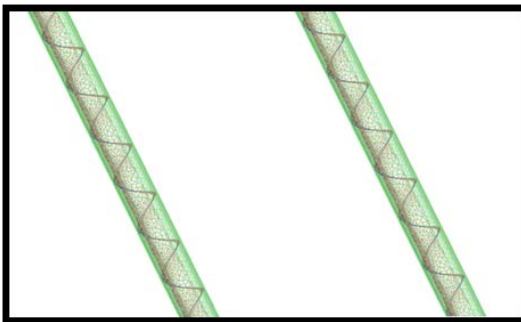
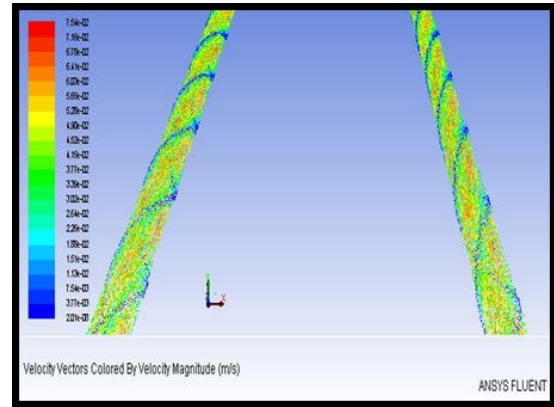
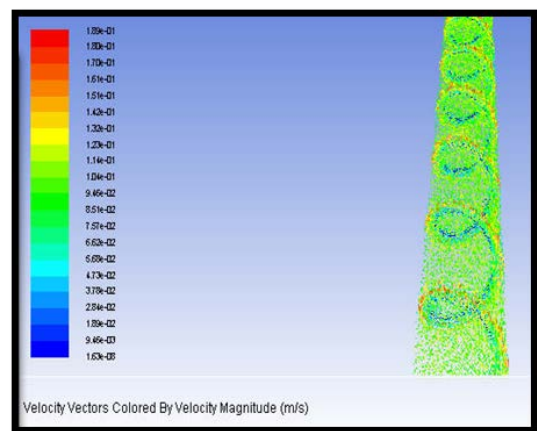


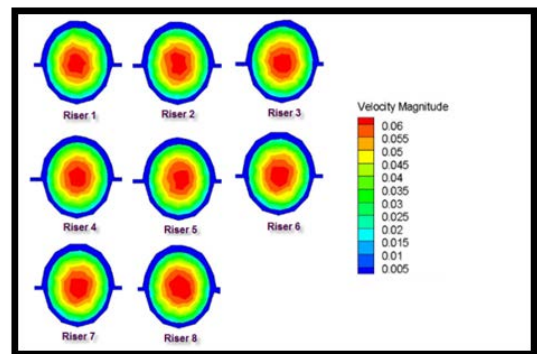
**Figure (7):** Volume mesh for helical spring surrounding solid shaft geometry inside riser pipe



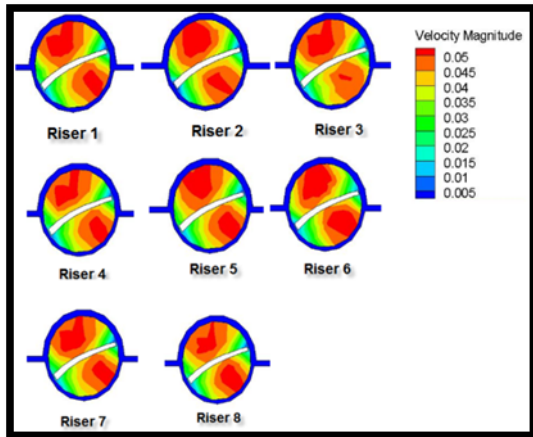
**Figure(8):** velocity vector of the water inside riser pipes with inserted twist strip at 100ℓ/hr. at solar noon.



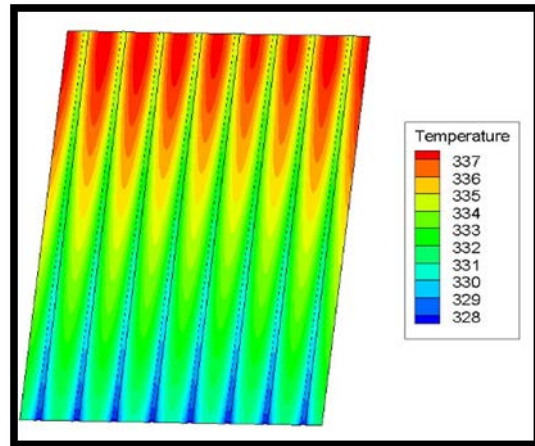
**Figure(9):** velocity vector of the water inside riser pipes with insert helical spring surrounding solid shaft at 100ℓ/hr. at solar noon



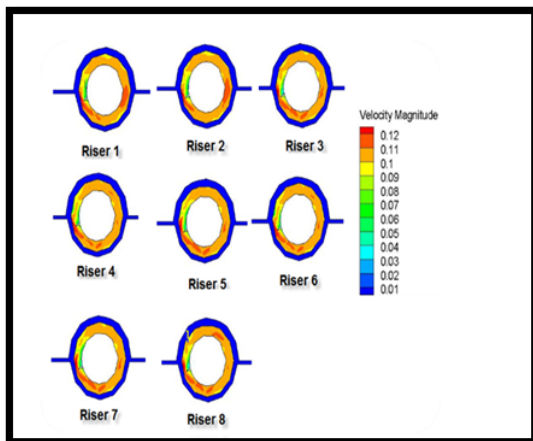
**Figure(10):** Velocity magnitude inside riser pipes without inserted device for the mass flow rate 100ℓ/hr. at solar noon



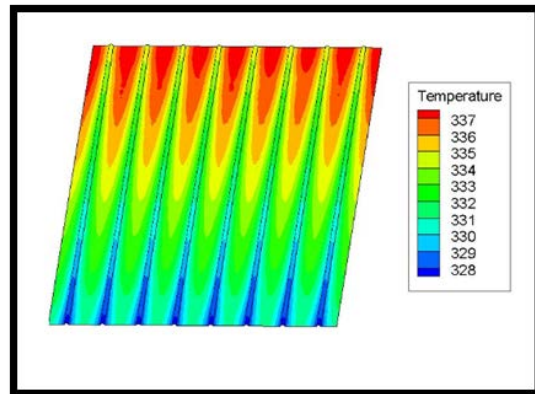
**Figure(11):** Velocity magnitude inside riser pipes with inserted twist strips for the mass flow rate 100ℓ/hr. at solar noon.



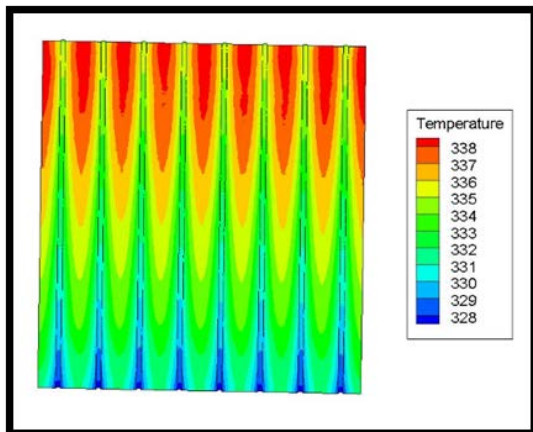
**Figure(14):** Temperature distribution of absorber plate with inserting twist strip inside riser pipes at solar noon at 100ℓ/hr.



**Figure(12):** Velocity magnitude inside riser pipes with inserted helical spring surrounding solid shaft for the mass flow rate 100ℓ/hr. at solar noon.



**Figure(15):** Temperature distribution of absorber plate with inserting helical spring inside riser pipes at solar noon at 100ℓ/h.



**Figure(13):** Temperature distribution of absorber plate without enhancement device at solar noon at 100ℓ/hr.

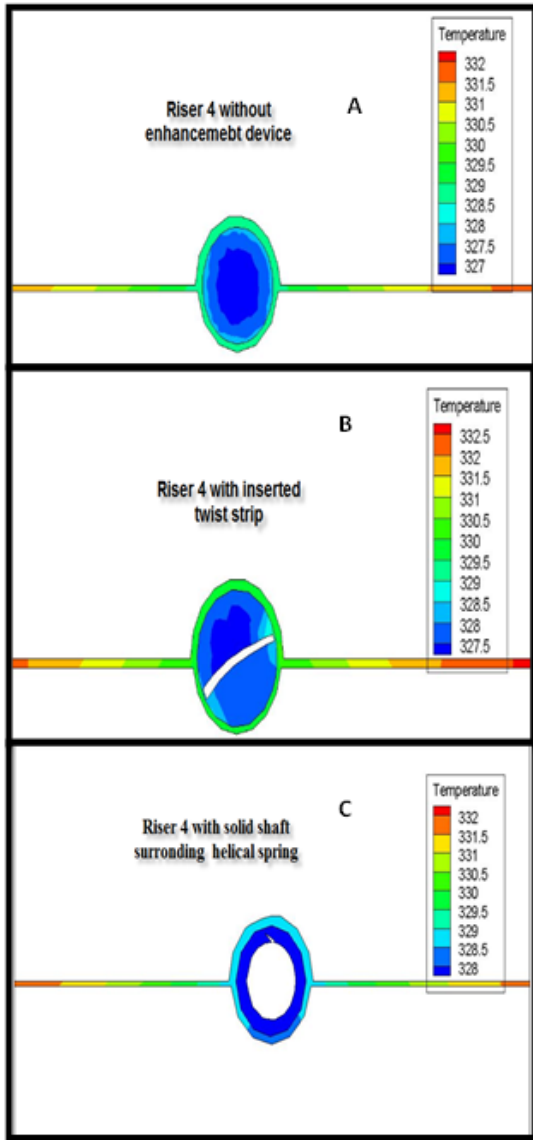


Figure (16): Temperature distribution of Z=10cm without and with enhancement device at 100l/hr.

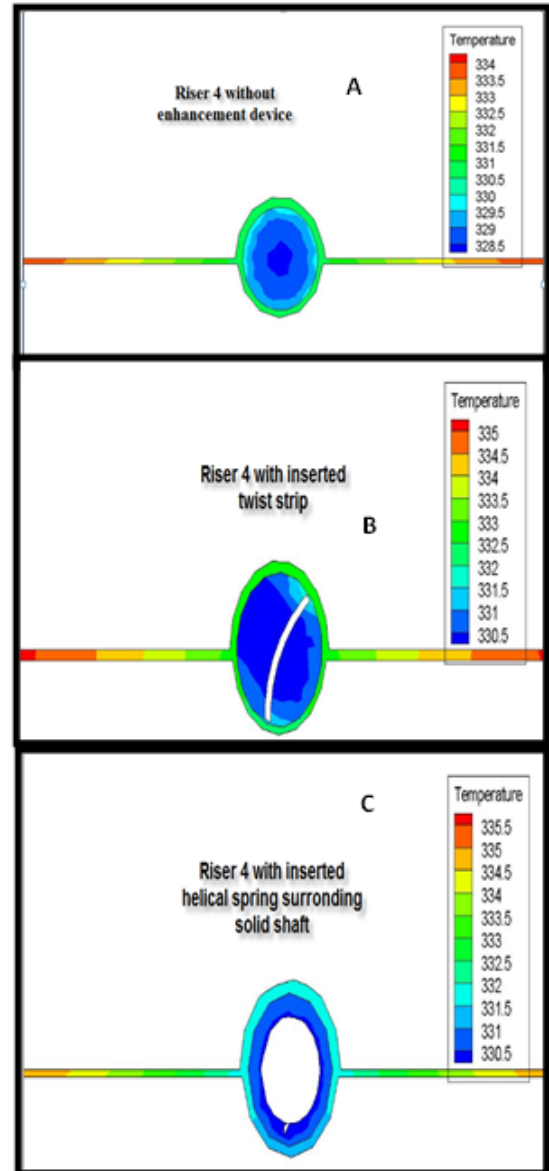
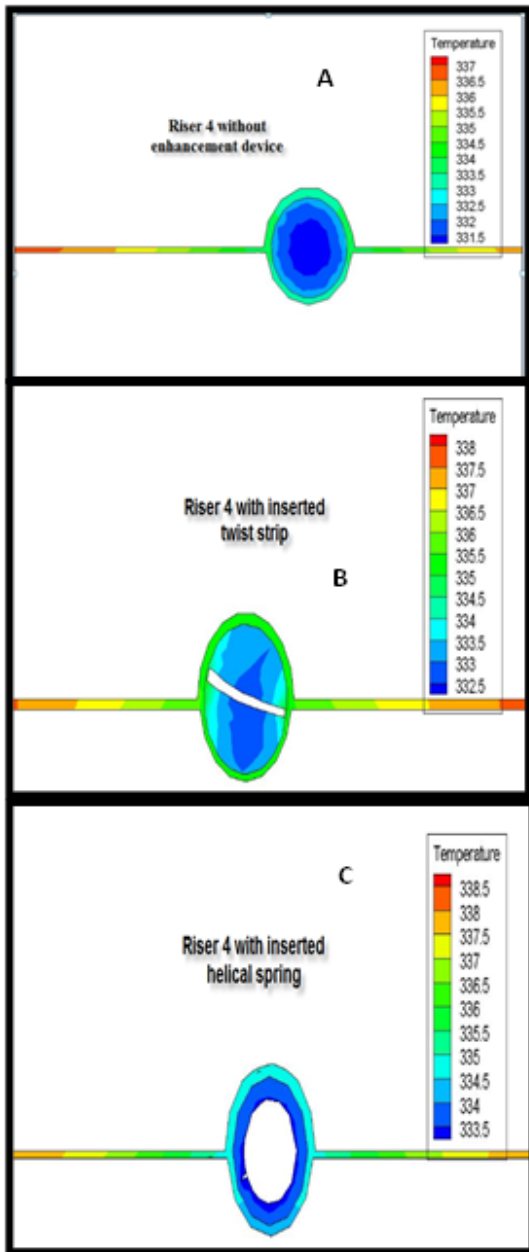
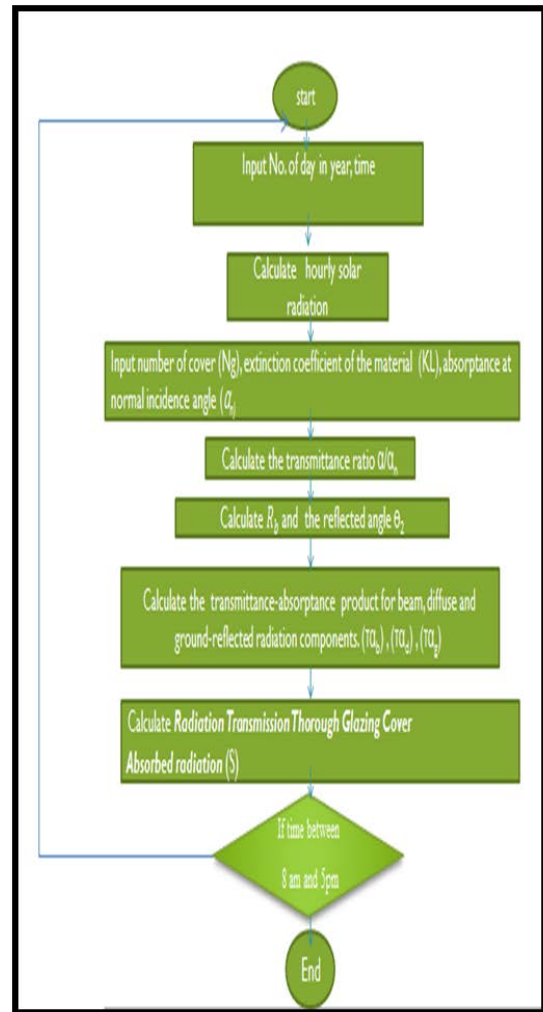


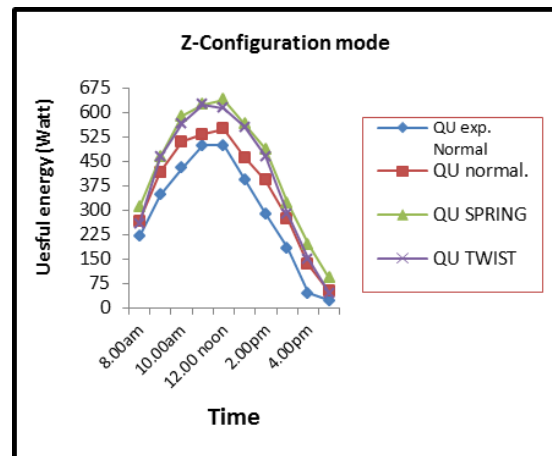
Figure (17): Temperature distribution of water inside riser at Z=50cm without and with enhancement device at 100l/hr.



**Figure(18):** Temperature distribution of water inside riser at Z=90cm without and with enhancement device at 100ℓ/hr.



**Figure(19):** Flow chart to calculate absorber energy.



**Figure(20):** Comparison between numerical and experimental results of flat plate solar water collectors with and without inserted device at 100 ℓ/hr.

## References

- [1] R. Herrero Marti'n, J. Pe'rez-Garci'a, A. Garc'a, "Simulation of an enhanced flat-plate solar liquid collector with wire-coil insert devices" *Solar Energy*, 455–469, 2011.
- [2] Chii-Dong Ho and Tsung-Ching Chen "Collector Efficiency of Double-Pass Sheet-and-Tube Solar Water Heaters with Internal Fins Attached" *Tamkang Journal of Science and Engineering*, Vol. 10, No. 4, pp. 323\_334, 2007.
- [3] Jaisankar, T.K. Radhakrishnan b,\*, K.N. Sheeba b, S. Suresh c "Experimental investigation of heat transfer and friction factor characteristics of thermosyphon solar water heater system fitted with spacer at the trailing edge of Left-Right twisted tapes" *Energy Conversion and Management* 50 ,2638–2649, 2009.
- [4] Alireza Hobbi a, Kamran Siddiqui a,b,\* Experimental study on the effect of heat transfer enhancement devices in flat-plate solar collectors" *International Journal of Heat and Mass Transfer* 52, 4650–4658, 2009.
- [5] Nagarajan , Nitesh Mittal and Rohit Chechani "Experimental studies on heat transfer and friction factor characteristics of parabolic trough solar water heating system with and without twisted tapes" *Proceedings of the 37th National & 4th International Conference on Fluid Mechanics and Fluid Power December 16-18, IIT Madras, Chennai, India, 2010.*
- [6] Manjunath M S K,Vasudeva Karanth ,N Yagnesh Sharma and Member IAENG "Three Dimensional Numerical Analysis of Conjugate Heat Transfer for Enhancement of Thermal Performance using Finned Tubes in an Economical Unglazed Solar Flat Plate Collector" July 6 - 8, London, U.K, 2011.
- [7] Alberto Garc'a , Ruth Herrero Martin and Jos'e P'erez-Garc'a " Experimental study of heat transfer enhancement in a flat-plate solar water collector with wire-coil inserts " *Applied Thermal Engineering* 61, 461-468, 2013 .
- [8] Withada Jedsadaratanachai and Amnart Boonloi "Effect of Twisted Ratio on Flow Structure Heat Transfer and Thermal Improvement in a Circular Tube with Single Twisted Tape" *Journal of Mathematics and Statistics* 10 (1): 80-91, 2014.
- [9] ANSYS FLUENT, Version 14.5, ANSYS Inc. 2013.
- [10] Patankar S.V. and D.B. Spalding, "A calculation procedure for heat, mass and momentum transfer in three-dimensional parabolic flows", *International Journal of Heat Mass Transfer*, vol. 15, p. 1787, 1972.
- [11] Duffie, J.A., Beckman, W.A "Solar Engineering of Thermal Processes", third ed. John Wiley & Sons, Interscience, New York., 2006.
- [12] ASHRAE, *Handbook of Fundamentals*, Atlanta: American Society of Heating, Refrigerating, and Air-Conditioning Engineers, Inc, 2005.
- [13] FAWAZ S. ABDULLAH, FIRAS A. ALI "Estimation the Effects of each Site Factors, and Optical Factors on Absorbed Solar Radation Value That Incident on a Flat Plate Solar Collector" ,*Journal of Theoretical and Applied Information Technology* July 2012. Vol. 41 No.2.
- [14] Maytham A. Jasim " Utilization of air-water solar collector system for space heating" M.s.c Thesis university of Technology 2014.
- [15] Mohammed Fowzi Mohammed " Study to enhance thermal performance of the risers in flat plate solar water collectors" Ph.D. Thesis university of Technology 2015.

## محاكاة ديناميكية الموائع الحسابية لتقنيات التحسين في مجمعات الماء الشمسية المسطحة

د. محمد فوزي محمد  
قسم الهندسة الميكانيكية  
الجامعة التكنولوجية

د. قصي جهاد عبد الغفور  
قسم الهندسة الميكانيكية  
الجامعة التكنولوجية

د. جعفر مهدي حسن  
قسم الهندسة الميكانيكية  
الجامعة التكنولوجية

### الخلاصة

يوضح البحث الحالي دراسة عددية لتحسين الاداء الحراري لمجمعات الماء الشمسية المسطحة. تمت الدراسة العددية بحل المعادلات الحاكمة (الاستمرارية ، الزخم والطاقة) لجريان طبقي ثلاثي الابعاد باستخدام برنامج ( Fluent 14.5 ) . تضمن الحل العددي دراسة تأثير الجريان وتوزيع درجات الحرارة لمجمعات الماء الشمسية من خلال اقحام ادوات (شريط ملتوي ذات نسبة التواء (3) ، محور صلب محاط بنايض حلزوني ) داخل انابيب رفع الماء ومقارنتها مع مجمع شمسي بدون اقحام ادوات داخل انابيب رفع الماء عند معدل تدفق (100) لتر/ ساعة. اظهرت النتائج العددية ان اقحام شريط ملتوي ذات نسبة الالتواء (3) ومحور صلب محاط بنايض حلزوني داخل انابيب رفع الماء تؤدي الى تحسين انتقال الحرارة بشكل ملحوظ عن الحالة بدون اقحام هذه الادوات . ان الطاقة المفيدة في حالة الشريط الملتوي اعلى بمقدار (10%) في حالة المجمع الشمسي بدون ادوات اقحام . كذلك في حالة اقحام محور صلب محاط بنايض حلزوني بلغت الزيادة في مقدار الطاقة المفيدة (6.8 %) عن حالة الشريط الملتوي و ( 16.2%) عن حالة المجمع الشمسي بدون ادوات اقحام عند نفس معدل التدفق.